

Design, Modelling and Parametric Analysis of a BLDC Motor in E-Bike to Predict Torque Range

K. M. Sahana^{a,*}, T. G. Keerthi^a, Y. Gouthami^a, B. N. Anush^b, S. Hooli Shwetha^b,
Anusha Vadde^a, and T. V. Meghana^a

^a Department of EE, Ramaiah University of Applied Sciences, Bengaluru, Karnataka, India

^b Emvega Technologies Private Limited (DPIIT Registered), Bengaluru, Karnataka, India

*e-mail: sahana.hospet@gmail.com

Received June 27, 2022; revised October 17, 2022; accepted November 15, 2022

Abstract—Electric vehicles (EV) are gaining importance eventually in the world, they are being replaced by the internal combustion (IC) vehicles starting from bikes, cars, heavy duty vehicles and aircrafts. IC engine in conventional vehicles is replaced with electric motor in EV's. The motor incorporated has to have high starting torque hence in this research work a BLDC motor is designed, simulated and studied to enhance the torque range in E-Bike application. A 2D model of BLDC motor is built in COMSOL Multiphysics 5.6 computational tool. The results obtained from the theoretical and COMSOL multiphysics computational tool are compared. At the end of the research work, a parametric study is carried out for variations in shape of slots, dimensions of slots, poles per phase, stator and rotor materials and a parametric analysis is conducted for the same. The torque range of 22.162 to 32.001 Nm is obtained by varying the parameters, which are validated with the theoretical calculations.

Keywords: electric vehicles, brushless direct current (BLDC) motor, torque, slot depth and slot shape

DOI: 10.3103/S1068371223020098

1. INTRODUCTION

A Brushless DC (BLDC) motor is an electronically commuted DC motor without brushes. The controller provides PWM signals, which control the speed and torque of the synchronous motor. The working principle of the motor is the same as in a Brushed DC motor. The Lorentz force law says that a current-carrying conductor experiences a force when it is placed in a magnetic field. As a result of the reactive forces, magnet experiences an equal and opposite force. A BLDC motor's current-carrying conductor remains static while the PM moves. When coils of stator are powered from the source, they become an electromagnet and start producing a rotating magnetic field in the air gap. Despite the supply given being DC, switching produces a trapezoidal shaped pulsating Dc voltage. Due to the force of contact between the electromagnet stator and PM rotor, the rotor continues to rotate. The phase winding are electrified as north and south poles when the windings are switched with PWM signals. Because the north and south poles of the PM rotor are in line with stator poles, the motor rotates. The BLDC is manufactured with permanent magnets mounted on rotor surface and current carrying conductors wound on to the stator slots. The electrical commutation is used to convert electrical energy into mechanical energy. BLDC motors are classified into two types

outer rotor motors and inner rotor motors. The only variation between the two is in its design, while operating principles remain same. Electric vehicles (EVs) can potentially eliminate fossil fuel use in the transportation industry. Electrification of the transportation industry can also results in better energy efficiency and lower pollution levels in the local area. In E-bikes, most of the motors used are BLDC motors; hence this paper works on building BLDC motors for the E-bike applications and enhances the motor's torque for smooth and efficient working of the E-bike.

Hanselman, D.C. et al. [1] has explained the essential features of motor operation and design in simple mathematical terms, provided design equations for radial and axial flux motors, and explained basic motor drive schemes. The measurement of the geomagnetic field by an underwater robot during a cruise was described by Zhang et al. [2]. Yildirim et al. [3] used numerical modeling based on a finite element approach to study the impact of both material and geometrical properties of surface-mounted PM on cogging torque of a BLDC motor (FEM). Shinoy et al. [4] have discussed design of a high-power radial flux Brushless DC motor for an electromechanical actuation system and also examine the design and analysis of a high-power radial flux Brushless DC motor for electromechanical actuation. Jeon et al. [5] investigated

Table 1. Materials applied on the model

Stator Material		Rotor material	
Stator Stamping	Stator Winding	Rotor Magnets	Rotor Shaft
Silicon Steel M-36	Copper	Neodymium N-52	Aluminum
• Electrical conductivity— 2.325581 [MS/m]	Electrical conductivity— 5.998×10^7 [S/m]	• Electrical conductivity— 1/1.4 [μohm-m]	• Electrical conductivity— 3.774×10^7 [S/m]
• Relative permeability—1	• Relative permeability—1	• Relative permeability—1	• Relative permeability—1
• Relative Permittivity—1	• Relative Permittivity—1	• Relative Permittivity—1	• Relative Permittivity—1

about loss distribution of a three-phase induction motor and a BLDC motor when running point-of-core material using FEA and testing. To increase motor efficiency, they had chosen a high-quality core material. According to Kwon et al., the BLDC motors use three core materials [6]. In the B–H curve, they are examined and analyzed for operating state. Each operating condition for core and copper loss was estimated and compared. Shane et al. [7] have discussed the significant advancements in hysteretic characterization and permeability modeling of ferromagnetic and ferrimagnetic materials. Nadolski et al. [8] developed a mechatronic system that included a battery of accumulators, a power electronic converter, and a three-phase winding BLDC motor with PM for use in electric cars. Alphonse et al. [9] conducted a thorough investigation on designing a Solar Powered BLDC motor-driven electric vehicle, which is one of the answers to the upcoming issue. The article by Racewicz et al. [10] describes the design and construction of a light two-wheeled vehicle with a 3 kW brushless DC motor. The vehicle is supported by a steel frame similar to a standard bicycle. Vadde et al. [11] have designed a 10 kW BLDC motor with suitable assumptions to analyse the efficiency and electromagnetic torque. The influence of rotor design has been analysed based on the parameters of torque and efficiency.

This research aims to design a Permanent Magnet (PM) Brushless Direct Current (BLDC) motor to enhance the torque range for E-bike. The parametric study is carried out for the various parameters as slot depth, slot design, material of stator and rotor.

2. DESIGN OF BLDC MOTOR

The literature review was done on the present Epbikes to know the power rating, speed, and torque of the e-bike on road. According to the literature review, a 3.3 kW rating of BLDC motor was considered for E-bike application. After fixing the motor's rating and speed, the motor's stamping was examined. The

geometrical parameters of the existing standard stampings were measured using Vernier Calipers, and the design calculation was carried out to obtain the torque and efficiency based on the textbook by J.R. Hendershot et al. [16]. For the calculations obtained, the 2D model was built using the computational tool COMSOL 5.6 for the exact stamping measurements.

The model has mainly two parts rotor and stator. The stator part consists of slots, windings and the rotor part consists of magnets and a shaft. After the completion of the model, it was simulated to obtain the torque, rotor losses and stator losses. The Table 1 explains the materials considered for designing the 2D model.

The torque obtained in the simulation was analysed and compared to the theoretical model. The variation in geometrical parameters and materials of the stator, rotor, and shaft were made to improve the torque. The same model was implemented in COMSOL 5.6 multi-physics computational tool; the results obtained were compared with theoretical calculations.

2.1 Design Calculations

The fixed parameters are classified into three types: geometric, magnetic, and electrical. Outer stator radius, outer rotor radius, stator inner radius, and rotor inner radius are the fixed parameters throughout the optimization and the geometric parameters like tooth width, slot width, slot opening, the width of slot bottom, and back iron width are considered for variations during the optimization. In magnetic parameters, back iron flux is considered, while torque, resistance, inductance, back emf, and current all come under electrical parameters [1]. In order to find out the torque and efficiency calculations, some parameters were measured using the given stamping, and some were assumed. Figure 2 represents the block diagram of air gap flux magnetic density that is required to calculate torque in Eq. (1) for theoretical calculation.

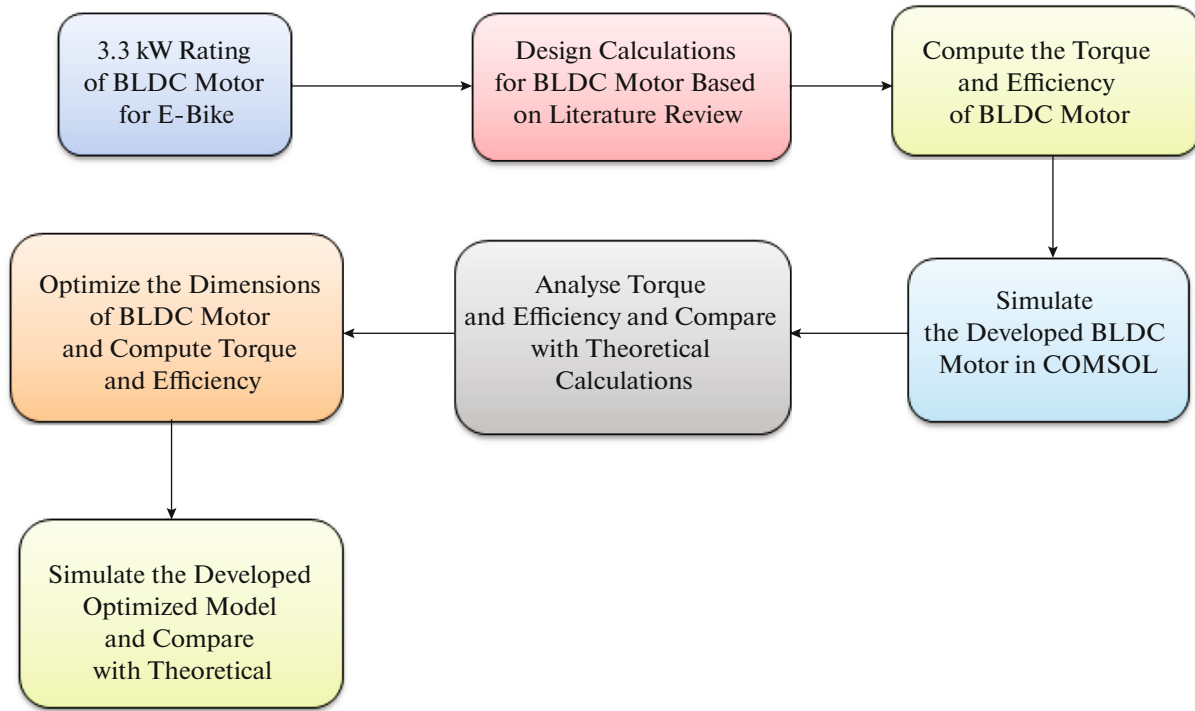


Fig. 1. Block diagram of the work.

tions and also efficiency is calculated from torque is presented in Eq. (2).

$$T = (N_m B_g L n_s i) R_{ro}, \quad (1)$$

$$\eta = \frac{T \omega_m}{\omega_m P_r P_{cl} P_s} \times 100, \quad (2)$$

where, N_m is number of magnets, B_g is magnetic flux density, L is length of motor, n_s is number of turns per slot, i is current, R_{ro} is outer rotor radius, ω_m is speed of the motor, P_r is ohmic power loss, P_{cl} is core losses and P_s is stray losses. As mentioned in Fig. 2 magnetic fraction has two different flux distributions one is radial flux distribution and the other is axial flux distribution. Based on review of literatures it was found that many of the BLDC motors uses radial flux distribution and its value obtained should be less than 1, in order to obtain appropriate torque [1]. Table 2 represents the parameters considered for both the torque and efficiency calculations.

The torque and efficiency obtained from theoretical calculations using Eq. (1) and Eq. (2) are 29.10 Nm and 65.68% respectively.

2.2 Two-Dimensional BLDC Motor Model

This section explains the design of 2D model in computational tool and various slot designs of stator is addressed.

Stator

The stator model was constructed in the computational tool, as shown in Fig. 3a. The slots are the stator's main parts, which were built as shown in Fig. 3a and were optimized for different dimensions to obtain better torque. The dimensions of the stator were considered according to the provided stampings. The dimensions of slots were considered as per Table 2.

Rotor

Rotor was also constructed in a computational tool, as shown in Fig. 3b. The magnets are the main parts of the rotor which were built as shown in Fig. 3b and were optimized for different dimensions to obtain better torque. The dimensions of the rotor were considered according to the stamping given, fixing the air gap to be 0.5 mm, and the dimensions of magnets were considered accordingly to obtain the best results, which are mentioned in Table 2.

Equations:

The physics chosen for building the model is magnetic fields which contain Infinite Element Domain, Magnetic Insulation, Ampere's Law and coils. The formulas used in the physics are:

$$\vec{B} = \mu_0 \mu_r \vec{H}, \quad (3)$$

$$\vec{J}_c = \sigma \vec{E}, \quad (4)$$

$$\vec{D} = \epsilon_0 \epsilon_r \vec{E}, \quad (5)$$

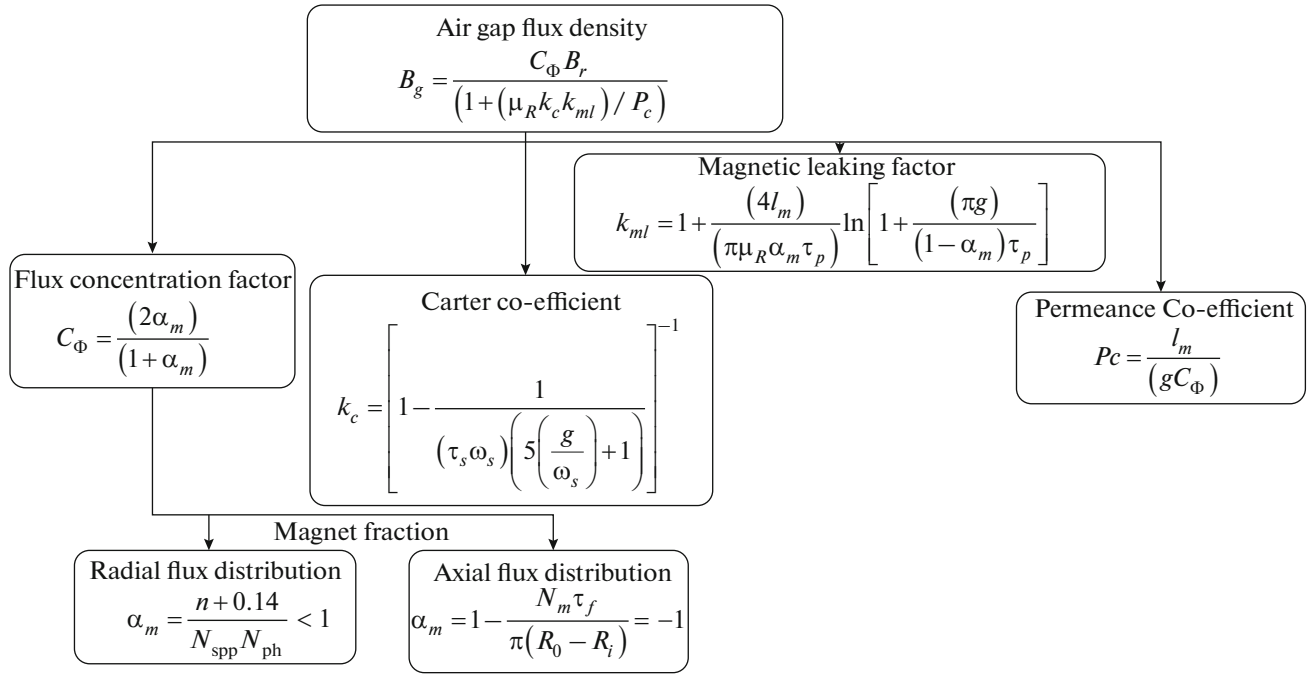


Fig. 2. Block diagram for air gap magnetic flux density.

where \vec{B} is magnetic field density, μ_r is relative permeability, μ_0 is permeability of free space, σ is electrical conductivity, ϵ_r is relative permittivity, ϵ_0 is permittivity in free space, \vec{E} is electric field strength, \vec{H} is mag-

netic field strength, \vec{J}_c is electric current density at a point, \vec{D} is displacement of electric field density and μ_r , ϵ_r and σ are taken from the material. To calculate the torque the rectangular coordinate system is con-

Table 2. Parameters for calculation of torque and efficiency

Measured Parameters	Given Parameters	Assumed Parameters
Radius inside stator, $R_{si} = 0.0475$ m	Voltage, $V = 75$ V	Number of slots, $N_s = 24$
Radius outside stator, $R_{s0} = 0.0825$ m	Current, $I = 30$ A	Air gap length, $g = 0.0005$ m
Radius outside rotor, $R_{ro} = 0.047$ m	Number of phase, $N_{ph} = 3$	Slot width, $w_{si} = 0.0051$ m
Outside stator, $R_{sb} = 0.0645$ m	Number of stator slots per phase, $N_{sm} = 8$	Slot opening, $w_s = 0.0025$ m
Back iron width, $w_{bi} = 0.018$ m	Number of slots per phase, $N_{sp} = \frac{N_s}{N_{ph}} = \frac{24}{3} = 8$	Width of slot bottom, $w_{sb} = 0.0127$ m
Width of slot, $w_t = 0.006$ m		Radius inside rotor, $R_{ri} = 0.040$ m
Tooth width, $w_{tb} = 0.004$ m		Number of magnets, $N_m = 16$
Depth of slot, $d_1 = 0.001$ m		Length of motor, $L = 0.15$ m
Depth of slot, $d_2 = 0.001$ m		Speed, $\omega_m = 3000$ rpm
Total slot depth, $d_s = 0.012$ m		Back EMF, $E_{max} = 70$ V
Width of magnet, 16.5 mm		
Length of magnet, 5 mm		
Height of magnet, 50 mm		
Depth of slot, $d_3 = 0.01$ m		

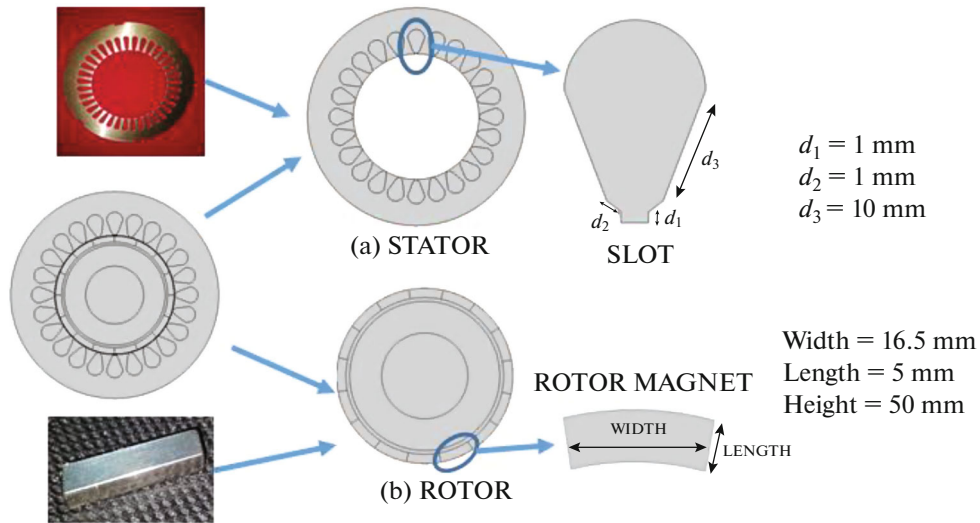


Fig. 3. 2D model of BLDC motor: model-1, (a) stator, (b) rotor.

verted to cylindrical coordinate system in computational tool for observing the torque.

3. PARAMETRIC STUDY

In order to improve the torque other design were adopted in the slot shape. This section discusses about the variation in the slot depth, variations in the slot shape and materials of the stator and rotor.

3.1. Variation in Slot Design

After obtaining the torque for model-1, the shape of slots are built, as shown in Figs. 4a, 4b, were designed to improve the torque of BLDC motor. The variation in the slot shapes design represents the improved torque compared to the previously built model-1, increasing the load capacity of the considered BLDC motor. The slot shape and dimensions were changed to increase the torque.

3.2. Slot Depth

In order to obtain better torque and efficiency for different design of model-1, model-2 and model-3 variation in the slot shape is done by changing a few parameters, such as the depth of the slot. Considering the depth of the slot, the theoretical output torque will not affect. Therefore the obtained torque remains the same as 29.10 Nm, whereas the change in the total slot depth affects the slot cross-sectional area and hence efficiency. After obtaining the torque for the variation in the slot shape, as conveyed in Fig. 4 model-2. One more model-3 was built, as shown in Figs. 5a, 5b. The variation in the slot shape for model-2 and model-3 represents the improved torque of 38.15 and 32.039 Nm respectively, compared to the previously built model-1, hence increasing the load capacity of the considered BLDC motor. The computation of slot area is tabulated in Table 3. The parametric study has been carried out to observe the changes in the torque and efficiency of the 2D model of the 3.3 kW BLDC motor.

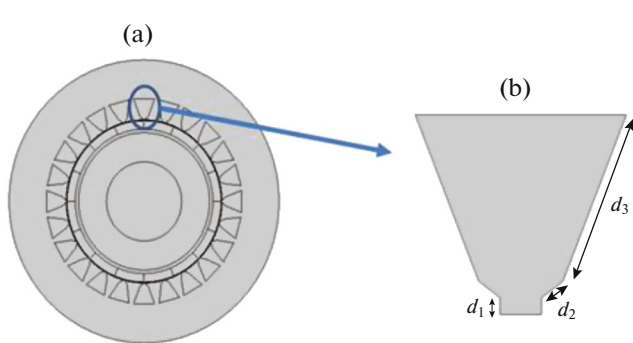


Fig. 4. (a) Model-2 BLDC motor, (b) shape of the slot.

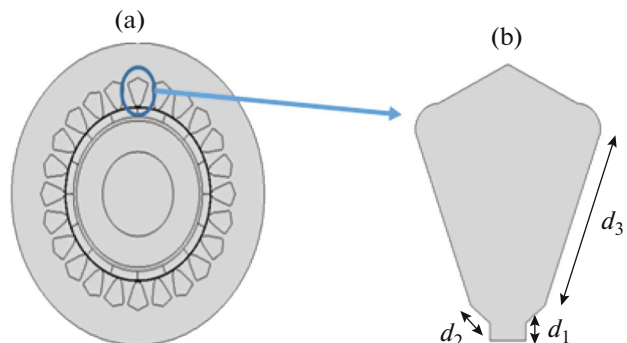










Fig. 5. (a) Model -3 of BLDC motor, (b) shape of the slot.

Table 3. Computation of slot area

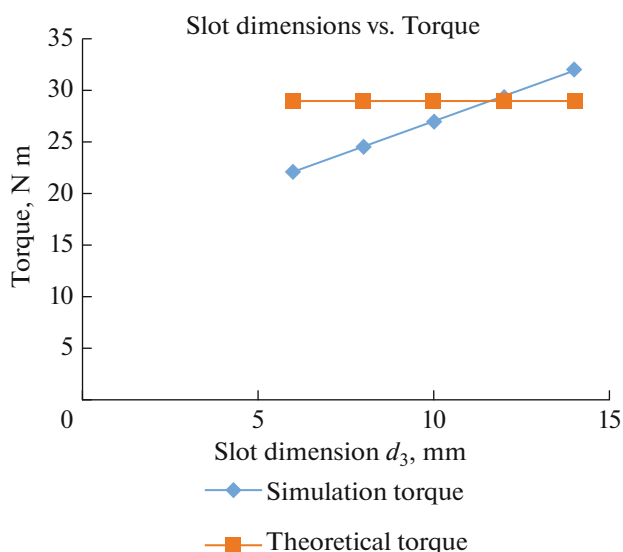
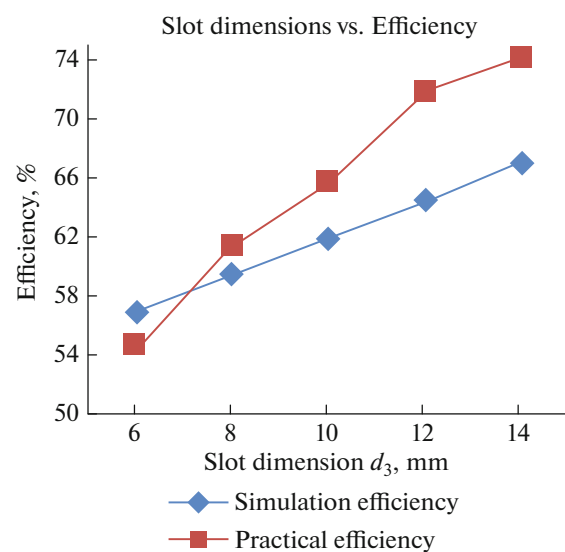
Model number	Slot shape	Slot Area	Slot area
Model 1	 $d_1 = 1 \text{ mm}$ $d_2 = 1 \text{ mm}$ $d_3 = 10 \text{ mm}$	 $A = \pi r^2 / 2$	0.157 m ²
		 $A = 1/2 h (a + b)$	
Model 2	 $d_1 = 1 \text{ mm}$ $d_2 = 1 \text{ mm}$ $d_3 = 10 \text{ mm}$	 $A = 1/2 h (a + b)$	0.09315 m ²
Model 3	 $d_1 = 1 \text{ mm}$ $d_2 = 1 \text{ mm}$ $d_3 = 10 \text{ mm}$	 $A = 1/2 b h$	0.05764 m ²
		 $A = 1/2 h (a + b)$	

3.3. Results

The Figs. 6 to 12 exhibits the results of motor modelled with the variation in slot depth d_3 , the shape of the slot, material of stator, the material of rotor and number of magnetic poles.

Figure 6 shows the comparison plot of simulation and resultant theoretical torque obtained for the

change in the slot dimension d_3 . The depths of the slot, d_3 values are varied from 6 to 14 mm. The theoretical calculation does not depend on the change in slot dimension, whereas the simulation results for torque is reduced as the d_3 value increases due to the reduction in back iron width this happens due to the materials assigned for the simulation. Figure 7 conveys the plot

**Fig. 6.** Torque vs. slot dimension d_3 .**Fig. 7.** Slot dimensions vs. efficiency.

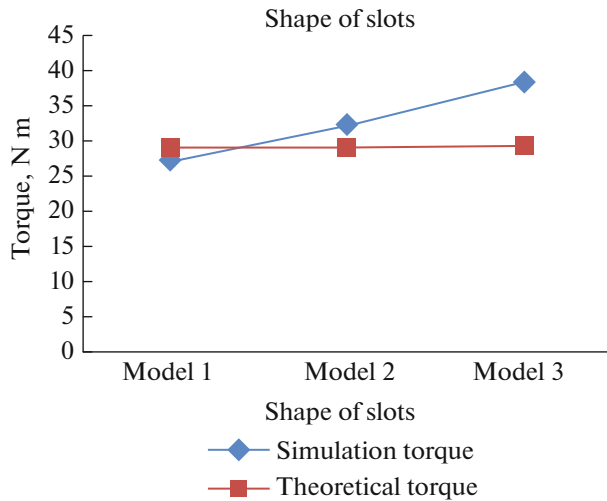


Fig. 8. Torque vs. shape of slots.

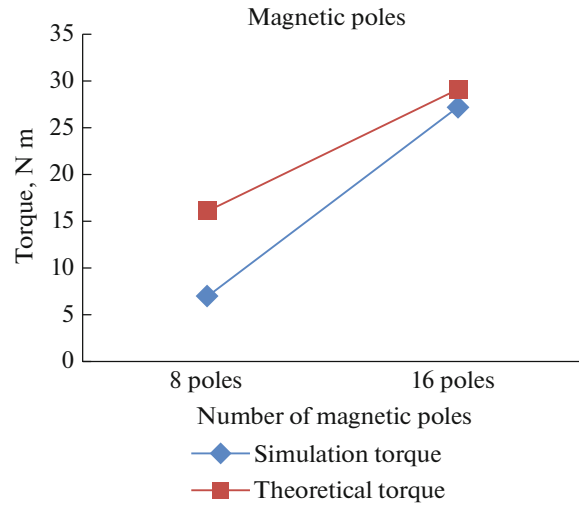


Fig. 9. Torque vs. number of magnetic poles.

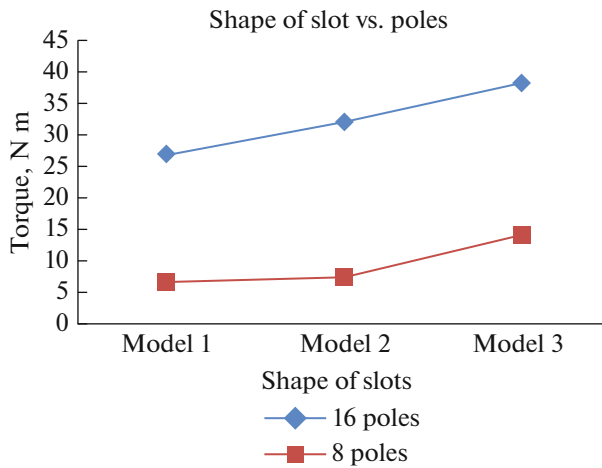


Fig. 10. Shape of slots vs. number of poles.

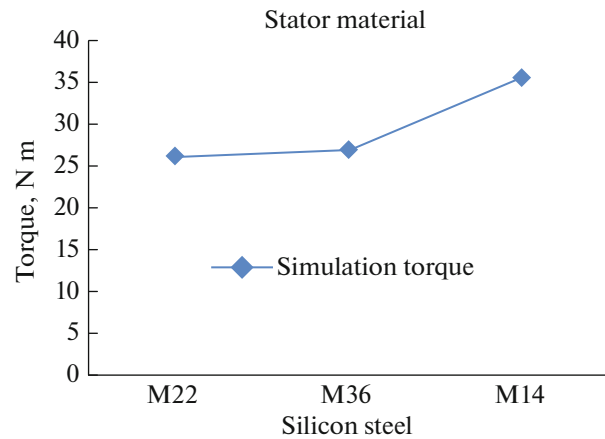


Fig. 11. Torque vs. stator material.

obtained for the model's efficiency with the change in the slot dimension d_3 . The depths of the slot, d_3 values are varied from 6 to 14 mm. The plot represents the efficiency for the simulation results are increasing with the increase in the d_3 value due to the decrease in stator losses, reduction in back iron width and the theoretical efficiency increase with the increase in d_3 value due to the increase in conductor area. Figure 8 represents the torque for the changes in the shape of slots. The shapes of the slots considered are as represented in model-1 and model-2. The shape of the slots does not affect the theoretical calculations; hence the plot shows a constant torque value. In contrast, the simulation results for torque can be seen increasing with the change in the shape of the slot Fig. 9 exhibits the comparison plot of the simulation and resultant theoretical torque achieved for the change in the number of magnetic

poles. The number of poles considered for this plot is 8 and 16. Both the theoretical and simulation results increase with the number of magnetic poles.

The rotor and stator material were not considered during the design calculations; hence the parametric study is done geometrical parameters only for the simulation results. Figure 10 represents the torque for the changes in the shape of slots vs. number of magnetic poles. The shape of the slots considered are as represented in model-1 and model-2, and the number of magnetic poles considered is 8 and 16. Both theoretical and simulation results depend on the change in the shape of the slots and the number of poles considered. Figure 11 exhibits the torque for the simulation results for the change in the stator material. The stator materials considered are silicon steel M22, M36, and M14. The simulation results show that a change in stator

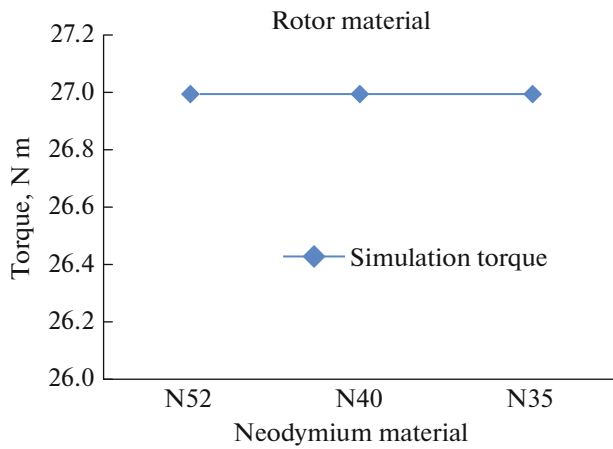


Fig. 12. Torque vs. rotor material.

material will affect the output torque. The theoretical result is independent of the material and slot depth of the model.

Figure 12 shows the torque for the simulation results for the change in the rotor material. The theoretical result does not depend on the material of the model. The rotor materials considered are neodymium N52, N40, and N35. The simulation results show that a change in rotor material will not affect the output torque, as the different grades of neodymium material used exhibits similar values of electric conductivity. To observe the effect of the change in slot depth d_3 the theoretical calculation and simulation is carried out by changing the d_3 for 7 to 15 mm. The results obtained for torque and efficiency with change in d_3 by the theoretical calculation and simulation are

represented in Table 4. The theoretically computed torque results are seen to be the same, since it is independent of slot depth. However, the motor's efficiency increases with an increase in slot depth since efficiency is dependent on slot area.

In order to obtain better torque and efficiency, variation in the slot dimension is done by changing the number of poles, N_m . Both torque and efficiency decreases since the number of poles is reduced to 8. The comparison is made between the calculated torques of BLDC motor with existing BLDC motor in E-bike of Ather model in Table 5.

CONCLUSION

This paper is on the design of a BLDC motor for the E-bike application, to enhance the motor's torque for smooth and efficient working. The theoretical calculations were made according to the given stamping, and the torque obtained is 29.10 Nm, and the efficiency is 65.68% for 16 poles and 24 slots. For eight poles, the torque obtained is 15.16 Nm, and efficiency is 39%.

The parametric study was carried out to predict the torque range for the 3.3 kW BLDC motor. The parameters were changed, such as slot depth, shape of the slot, stator and rotor material respectively. The following points are emerged from parametric study are as follows:

- Variation in the slot depth d_3 does not show any affect in the theoretical torque calculation, whereas the variation in the slot depth affects the simulation torque output

Table 4. Comparison of torque and efficiency at various slot depths

Slot depth (d_3) in mm	Torque (T) in Nm		Efficiency (η) in %	
	theoretical (Eq. (1))	simulation	theoretical (Eq. (2))	simulation
6	29.10	22.162	54.68	56.86
8	29.10	24.539	61.3	59.45
10	29.10	26.99	65.68	62.01
12	29.10	29.476	71.85	64.529
14	29.10	32.001	74.13	66.99

Table 5. Comparison of torque and efficiency for different number of poles

Parameters	Designed BLDC Motor (Model 1)		Ather(reference needed) [12]	
	theoretical	simulation	450X model	450 plus model
Torque, Nm	29.10	26.99	22	26
Peak Power, kW	3.3	3.3	5.4	6

- The different slot shapes of model-2 and model-3 results in more torque compared to the torque obtained for model-1
- The different grades of stator material have the effect in the output torque, whereas the different grades of rotor material will not have any effect on torque obtained
- The efficiency of the BLDC motor also increases with the increase in the slot depth d_3 .

CONFLICT OF INTEREST

The authors declare that they have no conflicts of interest.

REFERENCES

1. Hanselman, D.C., *Brushless Permanent Magnet Motor Design*, Faculty and Staff Monograph Publications, vol. 231, The Writers' Collective, 2003, 2nd ed. https://digitalcommons.library.umaine.edu/fac_monographs/231
2. Zhang, X., Wen, J., Wang, W., and Sun, J., Leakage magnetic field of BLDCM based on comsolmultiphysics, *AIP Conf. Proc.*, 2017, vol. 1834, no. 1, p. 020022. <https://doi.org/10.1063/1.4981561>
3. Yildirim, M., Kurum, H., Miljavec, D., and Corovic, S., Influence of material and geometrical properties of permanent magnets on cogging torque of BLDC, *Eng., Technol. Appl. Sci. Res.*, 2018, vol. 8, no. 2, pp. 2656–2662. <https://doi.org/10.48084/etasr.1725>
4. Shinoy, K.S., Sebastian, B., and Namboodiripad, M.N., Design of 100kW brushless DC motor for advanced actuation system using COMSOL, *Proc. 2016 COMSOL Conf.*, Bangalore, India, 2016.
5. Kwon, S.O., Lee, J.J., Lee, B.H., Kim, J.H., Ha, K.H., and Hong, J.P., Loss distribution of three-phase induction motor and BLDC motor according to core materials and operating, *IEEE Trans. Magn.*, 2009, vol. 45, no. 10, pp. 4740–4743. <https://doi.org/10.1109/TMAG.2009.2022749>
6. Jeon, Y.S., Mok, H.S., Choe, G.H., Kim, D.K., and Ryu, J.S., A new simulation model of BLDC motor with real back EMF waveform, *COMPEL 2000. 7th Workshop on Computers in Power Electronics*, Blacksburg, Va., 2000, IEEE, 2000, pp. 217–220. <https://doi.org/10.1109/CIPE.2000.904719>
7. Shane, G.M. and Sudhoff, S.D., Refinements in an-hysteretic characterization and permeability modeling, *IEEE Trans. Magn.*, 2010, vol. 46, no. 11, pp. 3834–3843. <https://doi.org/10.1109/TMAG.2010.2064781>
8. Nadolski, R., Ludwinek, K., Staszak, J., and Jaśkiewicz, M., Utilization of BLDC motor in electrical vehicles, *Przegl. Elektrotech.*, 2012, vol. 88, no. 4a, pp. 180–186.
9. Alphonse, I., Thilagar, H., and Singh, F.B., Design of solar powered BLDC motor driven electric vehicle, *Int. J. Renewable Energy Res.*, 2012, vol. 2, no 3, pp. 456–462. <https://doi.org/10.20508/ijrer.v2i3.260.g6045>
10. Racewicz, S., Kazimierczuk, P., Kolator, B., and Olszewski, A., Use of 3 kW BLDC motor for light two-wheeled electric vehicle construction, *IOP Conf. Ser.: Mater. Sci. Eng.*, 2018, vol. 421, p. 042067. <https://doi.org/10.1088/1757-899X/421/4/042067>
11. Vadde, A. and Sachin, S., Influence of rotor design in BLDC motor for two-wheeler electric vehicle, *1st Int. Conf. on Power Electronics and Energy (ICPEE)*, Bhubaneswar, India, 2021, IEEE, 2021, pp. 1–6. <https://doi.org/10.1109/ICPEE50452.2021.9358520>
12. Ather Energy, <https://www.atherenergy.com/>. Cited March 8, 2022.
13. Matsui, T. and Yun, K., Magnetic properties of silicon steel sheet core with different processing stress, *MATEC Web Conf.*, 2018, vol. 207, p. 03017. <https://doi.org/10.1051/mateconf/201820703017>
14. Uyar, O. and Cunkas, M., Torque and speed control of BLDC motor for pedelec, *5th Int. Conf. on Innovation in Science and Technology*, Barcelona, 2018, pp. 64–73.
15. Anshory, I., Robandi, I., Jamaaluddin, Fudholi, A., and Wirawan, Transfer function modeling and optimization speed response of BLDC motor e-bike using intelligent controller, *J. Eng. Sci. Technol.*, 2021, vol. 16, no. 1, pp. 305–324.
16. Yedamale, P., Brushless DC (BLDC) motor fundamentals, *Microchip*, 2003, vol. 20, no. 1, p. DS00885A.
17. Hendershot, J.R., and Miller, T.J.E., *Design of Brushless Permanent-Magnet Motors*, Magna Physics, 1994.